ISSN 1330-3651 (Print), ISSN 1848-6339 (Online)
https://doi.org/10.17559/TV-20210623123037
Original scientific paper

Development of Crystallization Calibration Model for Real-Time Monitoring of Fosamprenavir Calcium Particle Size Distribution

Hrvoje DORIĆ*, Nenad BOLF, Damir ŠAHNIĆ

Abstract: New approach in development of a calibration model for continuous monitoring of particle size distribution during crystallization of Fosamprenavir Calcium in a laboratory scale set-up is presented. Calibration models were developed based on data generated from Fosamprenavir Calcium crystallization experiments. The applicability of the method for continuous monitoring was explored comparing particle size distributions calculated from the developed model and particle size distributions determined by the laser light scattering method. Based on the calibration model of the particular process, partial least squares regression algorithm for continuous monitoring of particle size distribution was derived and applied and the results were validated. Presented method finds its application for real-time monitoring of particle size distribution, based on chord length distribution measurements.

Keywords: calibration model; crystallization; partial least squares regression; particle size distribution; real-time monitoring

1 INTRODUCTION

Crystallization is one of the most important but most challenging steps of obtaining various active pharmaceutical ingredients (API). The encouragement of FDA and other regulatory agencies related to the adoption and application of new advanced technologies for process monitoring and control [1] has been a relevant topic for more than two decades. Such methods are commonly applied for process optimization during process development, and to achieve the defined critical quality attributes (CQA's). The main advantage of process analytical technology (PAT) approach is a continuous insight into the process by measuring key process variables (concentration of dissolved substance, number of particles and particle size distribution (PSD), polymorphic form) and possibility to establish real-time control strategy [2].

PSD is a critical quality attribute for an API. Monitoring and real-time understanding of the PSD can play a crucial role in obtaining the desired physical properties of the product. Additionally, this information can increase the process robustness and minimize batch to batch variations. Real-time PSD can be monitored using focused beam reflectance measurement (FBRM). The output of the FBRM is the chord length distribution (CLD), which, for proper interpretation, needs to be correlated with PSD. If the measurement is performed in real-time, it is possible to monitor nucleation and crystal growth. The obtained data are useful for guiding and optimizing the crystallization process [3]. Various methods for converting CLD into PSD have been explained in the literature. Heath et al. [4] use theoretical and empirical relationships to calculate PSD. Li et al. [3] have developed an empirical model. Agimelen et al. [5] propose an algorithm for estimating the size and shape of needle-like particles from experimental CLD data. Petrak et al. [6] elaborated a statistical method that determined the particle shape from the measured CLD. A method that combines FBRM with image analysis is suggested by Agimelen et al. [7] for estimating particle size and shape. Pandit and Ranade [8] presented a mathematical model for a single particle that should simplify conversion of CLD into PSD. Irizarry et al. [9] proposed a method for prediction of one-dimensional and two-dimensional PSD based on the measured CLD. PSD can be determined by image analysis as explained in paper by Eggers et al. [10]. A different approach for describing the state of a crystallization system is proposed by Griffin et al. [11]. They suggest monitoring of the mass/number of particles ratio which gives an intuitive insight into the particles size. Paper by Szilagyi and Nagy [12] addresses the problem of the real-time simulation of the CLD and aspect ratio distribution (ARD). Pandit et al. [13] investigates a strategy for real-time monitoring of biopharma crystallization using FBRM to obtain real time CLD of crystals obtained using static and dynamic conditions.

In the presented research an empirical approach is used. Partial least squares regression (PLSR) [14] and principal component analysis (PCA) [15] were applied for data analysis and calibration model development. Recrystallization of Fosamprenavir Calcium (FSM-Ca) was conducted to obtain samples with different PSDs. CLD and PSD data were collected for model development. The main motivation was to develop a simple real-time PSD monitoring method which does not require deep insight into optical and physical properties of the system. Instead, it is based on collected laboratory CLD and PSD data for crystallization system of interest.

2 EXPERIMENTAL

2.1 Materials

API compound FSM-Ca ($C_{25}H_{34}CaN_3O_9PS$) was obtained from a pharmaceutical company. During FSM-Ca recrystallization process methanol (CH_3OH, min. 99,8%) was used as a solvent and water (H_2O) as an antisolvent. Later on, CLD data acquiring was conducted with recrystallized FSM-Ca suspended in antisolvent isopropanol ($(CH_3)_2CHOH$, min. 99,5%).

2.2 Equipment

CLD data was acquired using a Mettler Toledo FBRM G400 probe. PSD of the recrystallized FSM-Ca samples was determined by dry method using laser diffraction particle size analyzer Malvern Mastersizer 3000. Shape

and size of crystals were analysed by image analysis taken from optical microscope Olympus BX53M connected to PC. Recrystallization processes of FSM-Ca were performed in 1-liter jacketed glass reactor, an overhead mechanical agitator with a 4 blade 45° pitched blade turbine and a circulating Lauda PRO RP-245-E thermostatic bath. CLD data acquisition was conducted in Mettler Toledo Optimax 1001 1-liter glass reactor equipped with a FBRM immersion probe, temperature probe, overhead mechanical agitator and a Peltier cooling device.

2.3 Fosamprenavir Calcium Recrystallization

Six recrystallization experiments of FSM-Ca were performed in order to prepare samples with different PSDs. Recrystallization procedures can be seen and compared in Tab. 1. Varying the process conditions (cooling rate, seeding, antisolvent addition, mixing rate) resulted with 7 different PSD samples (including original sample) of FSM-Ca. Supersaturation and solubility curves were previously experimentally determined. Follows the procedure of one of the conducted recrystallization processes.

50 g of FSM-Ca was suspended in 500 mL of methanol (100 g/L) in 1-L reactor. Agitation was set to 180 RPM. Mixture was heated and maintained at 45 °C for 10 min. Afterwards, solution was filtered through blue filter paper on a Büchner funnel. During filtration methanol evaporates, so 37,5 mL of methanol was added to filtered solution in order to maintain initial concentration. Afterwards, the mixture was heated to 52 °C. Over 20 min 108 mL of water was dripped into the mixture. Temperature was maintained at 52 °C for 2 hours after observing first crystals. Suspension was then linearly cooled down to 22 °C with cooling rate of 0,0625 °C/min and maintained on the temperature for 15 hr with agitation set to 130 RPM. After this period suspension was filtered and crystals were washed with 0,1 L mixture of methanol and water (4:1). The product was dried under vacuum at 25 °C until the amount of moisture (Karl Fischer Moisture test, KF) is less than 13%.

Table 1 FSM-Ca recrystallization procedures for different samples

Step	FSM-Ca-1	FSM-Ca-2	FSM-Ca-3	FSM-Ca-4	FSM-Ca-5	FSM-Ca-6
1.	Add **50 g** FSM-Ca, 500 mL methanol into 1 L glass reactor; Set agitation to the **180 RPM**	Add **50 g** FSM-Ca, 500 mL methanol into 1 L glass reactor; Set agitation to the **200 RPM**	Add **30 g** FSM-Ca, 500 mL methanol into 1 L glass reactor; Set agitation to the **200 RPM**	Add **30 g** FSM-Ca, 500 mL methanol into 1 L glass reactor; Set agitation to the **200 RPM**	Add **20 g** FSM-Ca, 500 mL methanol into 1 L glass reactor; Set agitation to the **200 RPM**	Add **50 g** FSM-Ca, 500 mL methanol into 1 L glass reactor; Set agitation to the **200 RPM**
2.	Heat up mixture to 45 °C					
3.	Maintain temperature at 45 °C for **10 min**	Maintain temperature at 45 °C for **10 min**	Maintain temperature at 45 °C for **20 min**	Maintain temperature at 45 °C for **20 min**	Maintain temperature at 45 °C for **20 min**	Maintain temperature at 45 °C for **20 min**
4.	Filter solution through the blue filter paper over a Büchner funnel					
5.	Add filtered solution and 37,5 mL methanol into 1 L glass reactor					
6.	Heat up mixture to **52 °C**	Heat up mixture to **52 °C**	Heat up mixture to **45 °C**	Heat up mixture to **52 °C**	Heat up mixture to **52 °C**	Heat up mixture to **45 °C**
7.	Drip **108 mL** of water over **20 min** into mixture	Drip **97 mL** of water over **20 min** into mixture	Drip **96,25 mL** of water over **10 min** into mixture	Drip **70 mL** of water over **10 min** into mixture	Drip **70 mL** of water over **10 min** into mixture	Drip **96,25 mL** of water over **10 min** into mixture
8.	-	-	-	Cool down to **45 °C** and seed with **0,9 g FSM-Ca-0**	Cool down to **45 °C** and seed with **0,2 g FSM-Ca-0**	-
9.	Maintain temperature at **52 °C** for **2 hr** after observing first crystals	Maintain temperature at **52 °C** for **2 hr** after observing first crystals	Maintain temperature at **45 °C** for **1 hr** after observing first crystals	Maintain temperature at **45 °C** for **2 hr** after observing first crystals	Maintain temperature at **45°C** for **2 hr** after observing first crystals	Maintain temperature at **45°C** for **1 hr** after observing first crystals
10.	Linearly cool down to **22 °C** (cooling rate **0,0625 °C/min**)	Linearly cool down to **22 °C** (cooling rate **0,0625 °C/min**)	Linearly cool down to **15 °C** (cooling rate **0,125 °C/min**)	Linearly cool down to **15 °C** (cooling rate 0,1 °C/min)	Linearly cool down to **15 °C** (cooling rate **0,1 °C/min**)	Linearly cool down to **15 °C** (cooling rate **0,167 °C/min**)
11.	Maintain temperature at **22 °C for 15 hr; 130 RMP**	Maintain temperature at **22 °C for 15 hr; 200 RMP**	-	Maintain temperature at **15 °C for 15 hr; 200 RMP**	Maintain temperature at **15 °C for 15 hr; 200 RMP**	-
12.	Filter suspension and wash product with 0,1 L methanol-water mixture (MeOH:H20 = 4:1)					
13.	Dry at 25 °C under vacuum until KF < 13%					

2.4 Acquiring Chord Length Distribution Data

CLD data were acquired using FBRM G400 probe. Probe was installed above impeller at 45° angle. Sampling period of FBRM probe was 30 seconds. 2 grams of each recrystallized sample of FSM-Ca was suspended in 500 mL of isopropanol (antisolvent) in 1-L reactor (FSM-Ca 0,5% w/w) at constant temperature (10 °C) and monitored with FBRM probe. Although optical properties of isopropanol and methanol slightly differ, FSM-Ca was suspended in antisolvent to avoid any possibility of dissolution or crystallization. Amount of FSM-Ca sample was increased in 10 minute periods - 2 g of FSM-Ca was added to suspension to increase the quantity of sample, meanwhile CLD data was acquired. Amount of FSM-Ca sample was increased 10 times, up to the final concentration of FSM-Ca 5,3% w/w.

2.5 Multivariate Analysis and Calibration Model Development

CLD and PSD data sets for model development were acquired from 7 FSM-Ca crystalline samples with different PSDs. During gathering of CLD data for particular FSM-Ca samples, the quantity of crystalline sample in suspension was increased progressively to consider its possible influence on the resulting CLD. The aim was to increase the robustness of the developed model. To gain

insight into the data acquired CLD data was preprocessed and analysed using PCA (MathWorks MATLAB). Furthermore, outliers were detected and removed based on visual analysis in PCA space, Mahalanobis distance and leverage. Different structures of calibration models were developed using PLSR (MathWorks MATLAB) to establish relation between CLD and PSD data.

3 RESULTS AND DISCUSSION

3.1 CLD and PSD of Recrystallized FSM-Ca Samples

PSD data of the original and recrystallized samples is shown in Fig. 1. It can be seen that different recrystallization procedures resulted with different PSDs. Obtained CLD data for different FSM-Ca samples is shown in Fig. 2. For each sample, except FSM-Ca-6, there are 3 groups of curves where each group represents different amount of suspended FSM-Ca. High repeatability of CLD measurements for particular samples can be observed in Fig. 2. Multiple CLD curves of the same amount of particular FSM-Ca sample are almost completely overlapping. Also, it can be seen that sensitivity of the measurement for bigger particles is decreasing with higher amount of suspended crystalline material.

Fig. 3 shows results of sensitivity analysis of FBRM measurement when amount of crystalline sample is increasing.

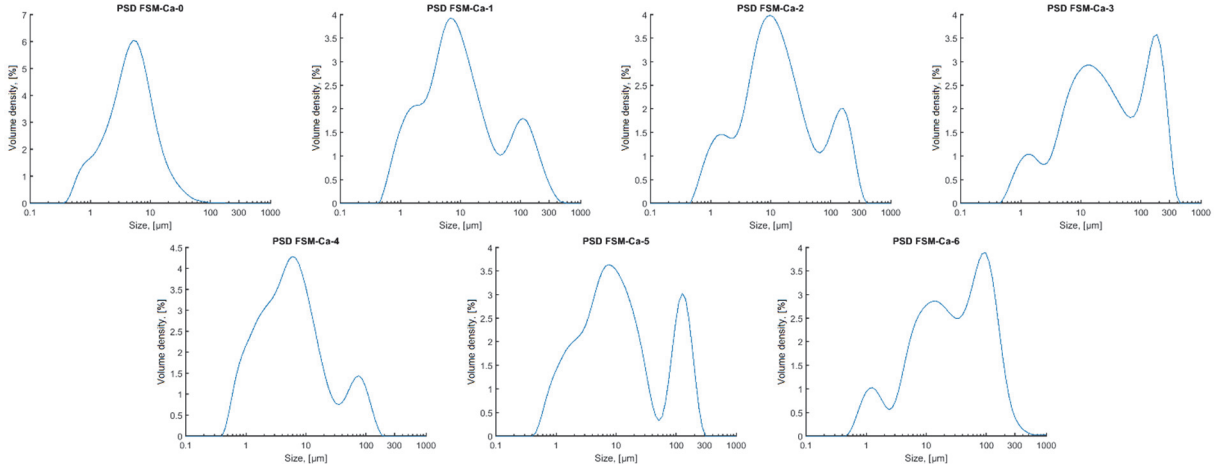

Figure 1 PSDs of original and recrystallized FSM-Ca samples

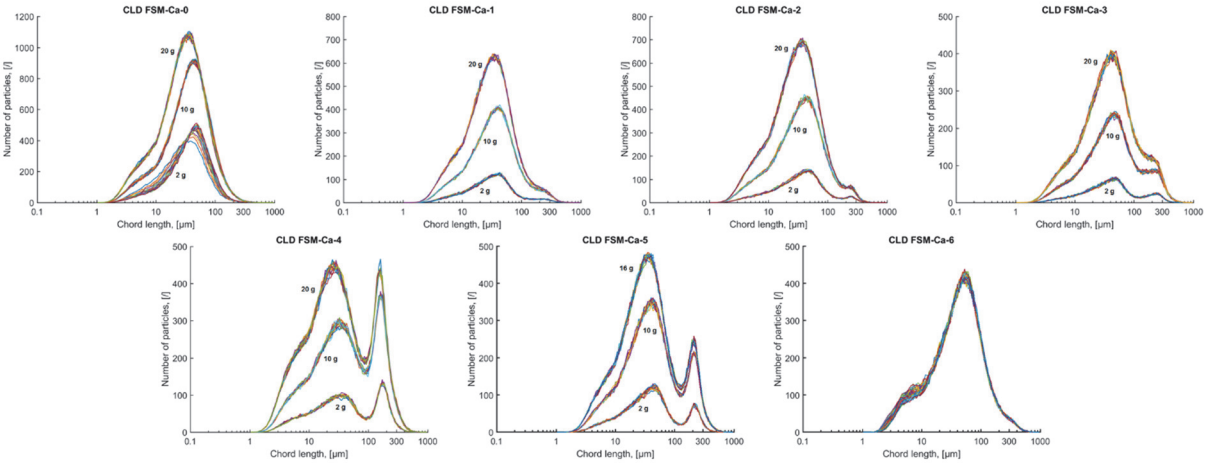

Figure 2 Original and recrystallized FSM-Ca samples CLDs

With increased amount of crystalline material in the suspension, the sensitivity of measurement is decreasing due to decreased "field of view" of FBRM probe which results with lower number of distinguishable counts. Microscopic images of original and recrystallized samples of FSM-Ca are shown in Fig. 4. While crystals of original FSM-Ca-0 sample are smaller and their dimensions are mostly similar, all recrystallized samples have needle-like shape of crystals with one dimension much bigger than the others. Also, it can be noted that the microscopic images are in accordance with PSDs shown in Fig. 1, since the highest percentage of small particles is in samples FSM-Ca-0 and FSM-Ca-4 which can also be seen on microscopic images.

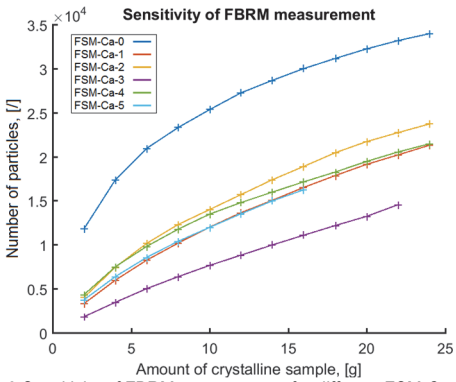

Figure 3 Sensitivity of FBRM measurement for different FSM-Ca crystalline samples

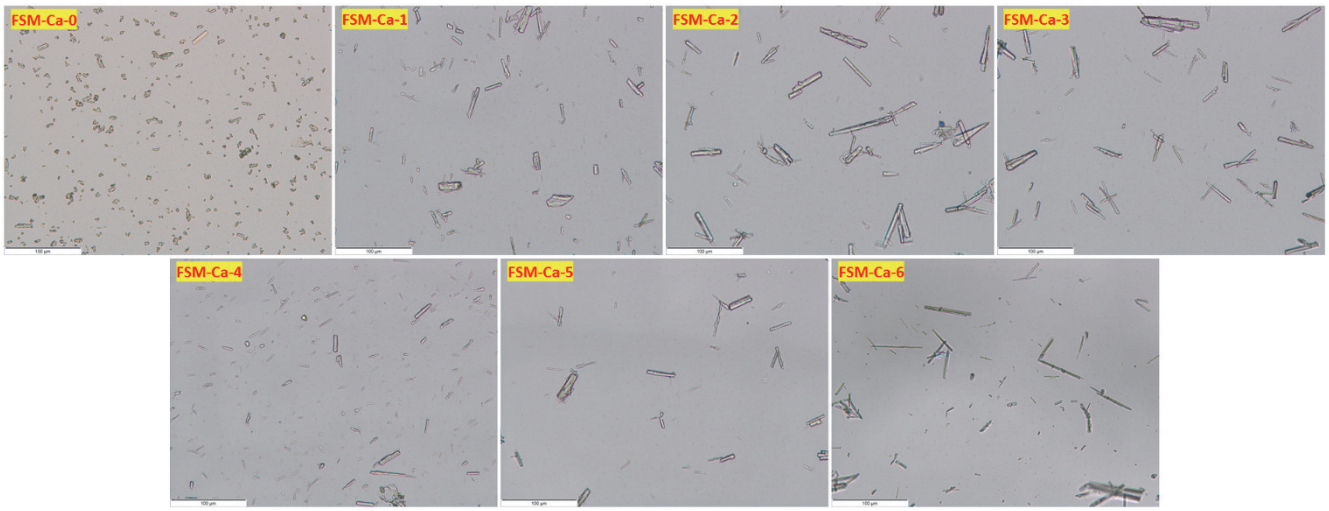

Figure 4 Microscopic image of original and recrystallized FSM-Ca samples

3.2 PCA Analysis of CLD Data

Each crystalline sample CLD data was individually analyzed. After outliers were detected and removed, the remaining data were combined and re-run through PCA.

Table 2 Explained variance in the first four principal components

Explained variance / %	PC-1	PC-2	PC-3	PC-4
FSM-Ca-0	71,36	14,09	1,66	1,25
FSM-Ca-1	79,66	5,50	2,18	2,02
FSM-Ca-2	83,31	5,86	1,72	1,23
FSM-Ca-3	84,06	4,29	2,35	1,71
FSM-Ca-4	81,93	8,33	1,29	1,15
FSM-Ca-5	88,08	2,79	2,17	1,20
FSM-Ca-6	52,12	21,84	5,02	4,28

Tab. 2 reveals that almost all variance in the data is explained by the first two components. The analysis of the loading vectors shows that PC-1 mainly describes the amount of crystalline sample in size classes with higher number, while PC-2 mostly describes the amount of crystalline sample in classes with lower number of observed particles. Loading vectors are arranged in the counter-clockwise manner with lower size classes starting in bottom-right quadrant and the highest size classes finishing in the upper-left quadrant.

Biplot charts of scores are shown in Fig. 5. In cases of smaller amounts of crystalline sample, the samples are arranged roughly vertically. For higher amounts of crystalline sample distinction between the different amounts is lost, and the samples are continuously arranged from (low PC-1, high PC-2) toward (high PC-1, low PC-2). Green marked samples are suspected as outliers. Most of outlier samples appear immediately after adding additional crystalline sample. Biplots of the scores reveal that samples with lower added crystalline sample have smaller PC-1 values, while they increase with addition of crystalline sample. PC-2 values depend on small differences in distributions of particles within size classes for particular crystalline sample added.

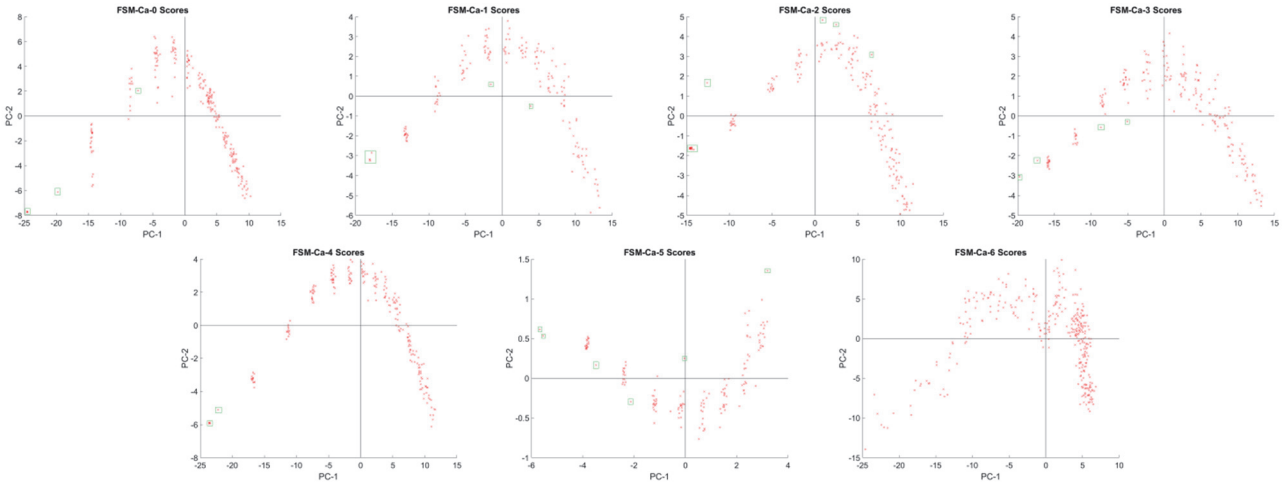

Figure 5 Biplots of FSM-Ca samples scores with marked outliers

3.3 Development of PLSR Calibration Model

During the model development few approaches were tested: dataset with and without outliers, scaled and unscaled dataset, as well as the effect of different number of PLSR factors. Cross-validation was performed for validating the model and evaluating the results using 10 Monte-Carlo iterations with 20% of data randomly left out in each iteration used for model testing. The models with the highest number of factors using unscaled and scaled data were developed to find out suitable number of factors for initial testing. Selected preliminary number of factors

was 20. Using unscaled data results with higher final value of explained variance in *Y* data. Also, lower number of factors is needed for achieving the same explained variance in *Y* data.

Table 3 R^2 parameter for models developed on different input datasets

R^2 parameter / %	Whole dataset, unscaled	Whole dataset, scaled	Without outliers, unscaled	Without outliers, scaled
cumulative	86,99	87,00	88,02	87,38
FSM-Ca-0	99,66	99,80	99,88	99,98
FSM-Ca-1	99,10	98,62	99,30	98,25
FSM-Ca-2	98,13	97,78	97,82	97,41
FSM-Ca-3	98,93	98,94	99,13	99,26
FSM-Ca-4	99,54	99,63	99,53	99,12
FSM-Ca-5	98,82	98,72	98,15	98,75
FSM-Ca-6	97,65	94,54	99,41	99,81

Four variants of models were developed, Fig. 6: a) complete unscaled dataset, b) complete scaled dataset, c) removed outliers with unscaled dataset, d) removed outliers with scaled dataset.

Calculated R^2s are shown in Tab. 3. R^2 was calculated for matching of one random picked PSD calculated using model with its given PSD in each crystalline sample. Also, cumulative R^2 was calculated for whole validation dataset. Fig. 6 compares measured vs. calculated PSD from four differently preprocessed datasets for crystalline sample FSM-Ca-1. More cases of data without outliers resulted with better fit. Scaling of the data does not affect the model performance significantly. Models developed from unscaled data require less PLS factors for achieving the same accuracy. Accordingly, unscaled data models were chosen for further analysis.

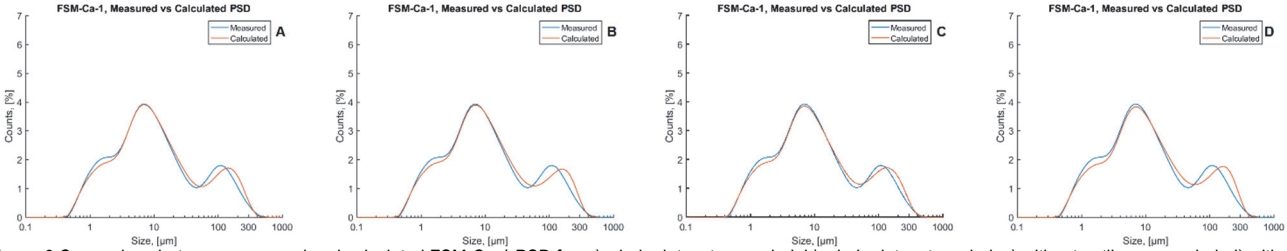

Figure 6 Comparison between measured and calculated FSM-Ca-1 PSD for: a) whole dataset, unscaled; b) whole dataset, scaled; c) without outliers, unscaled; d) without outliers, scaled

Table 4 R^2 parameter for models developed with different number of PLS factors

R^2 parameter / %	Number of PLS factors					
	10	9	8	7	6	5
cumulative	88,02	87,14	86,46	84,93	83,14	76,13
FSM-Ca-0	99,88	99,91	99,90	99,86	99,32	99,91
FSM-Ca-1	99,30	99,22	97,49	98,72	97,38	97,95
FSM-Ca-2	97,82	98,15	97,66	96,55	96,44	96,83
FSM-Ca-3	99,13	99,22	99,60	98,75	96,51	83,93
FSM-Ca-4	99,53	99,68	99,70	99,64	99,73	99,24
FSM-Ca-5	98,15	97,39	98,01	97,68	97,55	88,89
FSM-Ca-6	99,41	99,77	99,55	97,68	97,84	94,02

Finally, the impact of PLS factor number on model accuracy was examined on model with unscaled dataset with removed outliers. Number of PLS factors was altered to determine its impact on the model accuracy. The results for the models with 10 to 5 PLS factors are given in Tab. 4.

Using higher number of factors would lead to overfitting, while using less than six factors results with lower model accuracy. Smaller number of components results with lower R^2 for cumulative validation dataset. Significant increase in R^2 for samples FSM-Ca-3, FSM-Ca-5 can be seen when 6th factor is included in model which explains 3rd peak in data. Based on the statistics the recommended number of PLS factors is 6 to 8. Fig. 7 shows comparison between measured and calculated PSDs with 6 PLS factor model for all FSM-Ca samples. Simpler PSDs (FSM-Ca-0 and FSM-Ca-4) are well-predicted even with lower number of factors, while more complex PSD samples require higher number of factors.

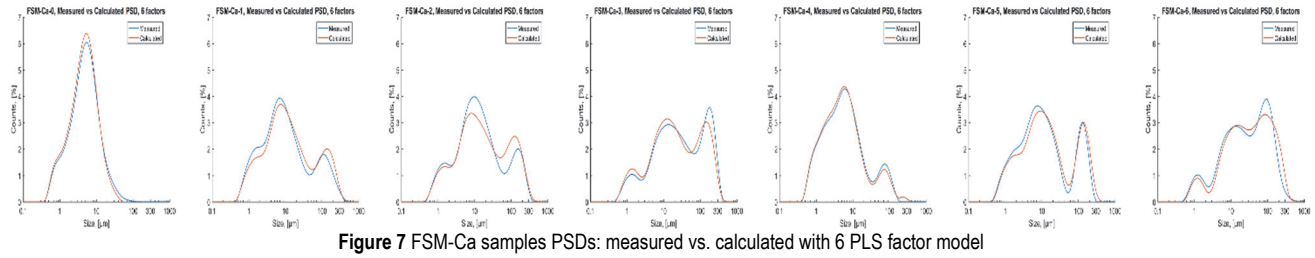

Figure 7 FSM-Ca samples PSDs: measured vs. calculated with 6 PLS factor model

Table 5 R^2 parameter for models developed with different number of PLS factors - test-set validation

R^2 parameter / %	Number of PLS factors					
	10	9	8	7	6	5
cumulative	88,67	86,97	90,89	92,29	90,94	71,58
FSM-Ca-0	97,07	96,79	95,98	98,30	97,34	98,32
FSM-Ca-1	95,61	96,13	96,18	95,36	95,32	95,71
FSM-Ca-2	93,19	93,16	92,28	87,81	87,53	80,91
FSM-Ca-3	64,50	58,58	66,47	63,34	70,77	57,29
FSM-Ca-4	0,00	0,00	0,00	0,00	0,00	0,00
FSM-Ca-5	70,96	72,97	72,26	77,50	79,47	82,33
FSM-Ca-6	88,67	86,97	90,89	92,29	90,94	71,58

During test-set validation for each sequence of validation one crystalline sample data was purposely omitted and later used for model testing. The results, shown in Tab. 5, were inferior since all data from single FSM-Ca sample was omitted during model development. It is obvious that models can predict PSD of FSM-Ca-0, FSM-Ca-1, FSM-Ca-2and FSM-Ca-6 with high accuracy. Models for FSM-Ca-3 and FSM-Ca-5 show lower accuracy, while sample FSM-Ca-4 cannot be predicted since the correlation between PSD and CLD for FSM-Ca-

4 evidently differs. Possible reason for that could be higher percentage of smaller particles in sample FSM-Ca-4 opposed to the other recrystallized samples, as can be seen in Fig. 4. Results of test-set validation for FSM-Ca samples with 6 PLS factors model are shown in Fig. 8.

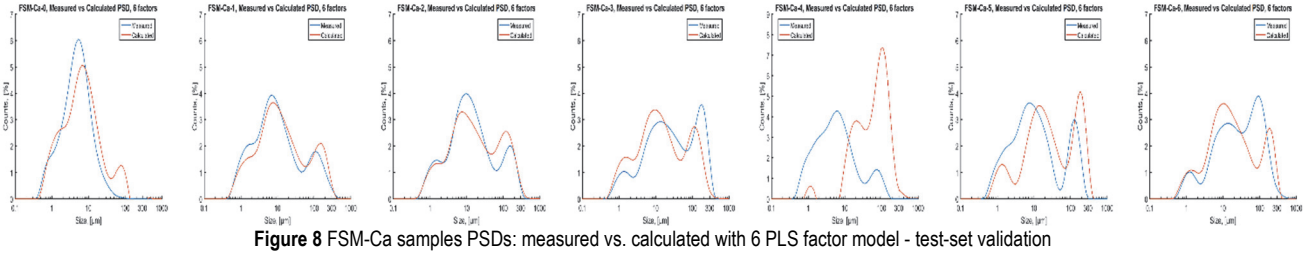

Figure 8 FSM-Ca samples PSDs: measured vs. calculated with 6 PLS factor model - test-set validation

4 CONCLUSION

PLSR calibration model for interpretation of PSD from measured CLD data for FSM-Ca is developed. The method is intended for real-time PSD monitoring and control in FSM-Ca crystallization process.

The main advantage of presented approach is in its simplicity, since to establish CLD to PSD correlation optical and physical properties of monitored solute-solvent system need not be known. The limitation is that it is only applicable to the particular system being analysed where the accuracy considerably depends on the data acquired for model development. A way for improvement would be acquiring crystalline samples during the crystallization process and using acquired data to improve the model performance. Possible nonlinearities in data-sets for other solute-solvent systems could be tackled by implementation of neural networks or similar nonlinear modelling techniques for development of calibration model.

Acknowledgements

This research is funded by European Structural and Investment Funds, grant number KK.01.1.1.07.0017 (CrystAPC - Crystallization Advanced Process Control).

5 REFERENCES

[1] US FDA (2004). Guidance for Industry. PAT - A Framework for Innovative Pharmaceutical Development, Manufacturing, and Quality Assurance

[2] Simon, L. L., Pataki, H., Marosi, G. et al. (2015). Assessment of recent process analytical technology (PAT) trends: A multiauthor review. *Organic Process Research & Development*, *19*, 3-62. https://doi.org/10.1021/op500261y

[3] Li, H., Kawajiri, Y., Grover, M. A., & Rousseau, R. W. (2014). Application of an empirical FBRM model to estimate crystal size distributions in batch crystallization. *Crystal Growth & Design, 14*, 607-616. https://doi.org/10.1021/cg401484d

[4] Heath, A. R., Fawell, P. D., Bahri, P. A., & Swift, J. D. (2009). Estimating average particle size by focused beam reflectance measurement (FBRM). *Particle & Particle Systems Characterization*, *19*, 84-95. https://doi.org/10.1002/1521-4117(200205)19:2<84::AIDPPSC84>3.0.CO;2-1

[5] Agimelen, O. S., Hamilton, P., Haley, I., Nordon, A., Vasile, M., Sefcik, J., & Mulholland, A. J. (2015). Estimation of particle size distribution and aspect ratio of non-spherical particles from chord length distribution. *Chemical Engineering Science*, *123*, 629-640. https://doi.org/10.1016/j.ces.2014.11.014

[6] Petrak, D., Dietrich, S., Eckardt, G., & Köhler, M. (2015). Two-dimensional particle shape analysis from chord measurements to increase accuracy of particle shape determination. *Powder Technology, 284*, 25-31. https://doi.org/10.1016/j.powtec.2015.06.036

[7] Agimelen, O. S., Jawor-Baczynska, A., McGinty, J., Dziewierz, J., Tachtatzis, C., Cleary, A., Haley, I., Michie, C., Andonovic, I., Sefcik, J., & Mulholland, A. J. (2016). Integration of in situ imaging and chord length distribution measurements for estimation of particle size and shape. *Chemical Engineering Science*, *144*, 87-100. https://doi.org/10.1016/j.ces.2016.01.007

[8] Pandit, A. V. & Ranade, V. V. (2016). Chord length distribution to particle size distribution. *AIChE Journal*, *62*, 4215-4228. https://doi.org/10.1002/aic.15338

[9] Irizarry, R., Chen, A., Crawford, R., Codan, L., & Schoell, J. (2017). Data-driven model and model paradigm to predict 1D and 2D particle size distribution from measured chord-length distribution. *Chemical Engineering Science*, *164*, 202-218. https://doi.org/10.1016/j.ces.2017.01.042

[10] Eggers, J., Kempkes, M., & Mazzotti, M. (2008). Measurement of size and shape distributions of particles through image analysis. *Chemical Engineering Science*, *63*, 5513-5521. https://doi.org/10.1016/j.ces.2008.08.007

[11] Griffin, D. J., Grover, M. A., Kawajiri, Y., & Rousseau, R. W. (2015, July). Combining ATR-FTIR and FBRM for feedback on crystal size. *2015 American Control Conference (ACC)*. https://doi.org/10.1109/acc.2015.7172006

[12] Szilágyi, B. & Nagy, Z. K. (2018). Aspect Ratio Distribution and Chord Length Distribution Driven Modeling of Crystallization of Two-Dimensional Crystals for Real-Time Model-Based Applications. *Crystal Growth & Design*, *18*, 5311-5321. https://doi.org/10.1021/acs.cgd.8b00758

[13] Pandit, A., Katkar, V., Ranade, V., & Bhambure, R. (2019). Real-Time Monitoring of Biopharmaceutical Crystallization: Chord Length Distribution to Crystal Size Distribution for Lysozyme, rHu Insulin, and Vitamin B12. *Industrial & Engineering Chemical Research, 58*, 7607-7619. https://doi.org/10.1021/acs.iecr.8b04613

[14] Wold, S., Sjöström, M., & Eriksson, L. (2001). PLS-regression: a basic tool of chemometrics. *Chemometrics and Intelligent Laboratory Systems*, *58*, 109-130. https://doi.org/10.1016/S0169-7439(01)00155-1

[15] Jolliffe, I. T. (2002). *Principal Component Analysis*. Springer Series in Statistics. New York: Springer-Verlag. https://doi.org/10.1007/b98835

Contact information:

Hrvoje DORIĆ, MS
(Corresponding author)
University of Zagreb,
Faculty of Chemical Engineering and Techology,
Marulićev trg 19, 10 000 Zagreb, Croatia
E-mail: hdoric@fkit.hr

Nenad BOLF, PhD, Professor
University of Zagreb,
Faculty of Chemical Engineering and Techology,
Marulićev trg 19, 10 000 Zagreb, Croatia
E-mail: bolf@fkit.hr

Damir ŠAHNIĆ, PhD
PLIVA Croatia Ltd. (member of TEVA group),
Prilaz baruna Filipovića 25, 10000 Zagreb, Croatia
E-mail: damir.sahnic@pliva.com